

## Impaired mitochondrial ketone body oxidation in insulin resistant states

Elric Zweck<sup>1,2,3,4,\*</sup>, Sarah Piel<sup>3,4,\*</sup>, Johannes W. Schmidt<sup>3,4</sup>, Daniel Scheiber<sup>1,2,3,4</sup>, Martin Schön<sup>1,2,5</sup>, Sabine Kahl<sup>1,2,5</sup>, Volker Burkart<sup>1,2</sup>, Bedair Dewidar<sup>1,2</sup>, Ricarda Remus<sup>3,4</sup>, Alexandra Chadt<sup>2,6</sup>, Hadi Al-Hasani<sup>2,6</sup>, Lucia Mastrototaro<sup>1,2</sup>, Hug Aubin<sup>4,7</sup>, Udo Boeken<sup>7</sup>, Artur Lichtenberg<sup>4,7</sup>, Jörg Distler<sup>8</sup>, Amin Polzin<sup>3,4</sup>, Malte Kelm<sup>3,4</sup>, Ralf Westenfeld<sup>3,4</sup>, Robert Wagner<sup>1,2,5</sup>, Patrick Schrauwen<sup>1,2</sup>, Julia Szendroedi<sup>1,2,9,10</sup>, Michael Roden<sup>1,2,5,§</sup>, Cesare Granata<sup>1,2,§,§</sup>

<sup>1</sup>Institute for Clinical Diabetology, German Diabetes Center, Leibniz Center for Diabetes Research, Heinrich-Heine-University Düsseldorf, Düsseldorf, Germany

<sup>2</sup>German Center for Diabetes Research (DZD e.V.), Partner Düsseldorf, Munich-Neuherberg, Germany

<sup>3</sup>Department of Cardiology, Pulmonology, and Vascular Medicine, Medical Faculty, Heinrich-Heine-University Düsseldorf, Düsseldorf, Germany

<sup>4</sup>CARID, Cardiovascular Research Institute Düsseldorf, Medical Faculty, Heinrich-Heine-University Düsseldorf, Düsseldorf, Germany

<sup>5</sup>Department of Endocrinology and Diabetology, Medical Faculty, Heinrich-Heine-University Düsseldorf, Düsseldorf, Germany

<sup>6</sup>Institute for Clinical Biochemistry and Pathobiochemistry, German Diabetes Center, Leibniz Center for Diabetes Research at Heinrich-Heine-University Düsseldorf, Düsseldorf, Germany

<sup>7</sup>Department of Cardiac Surgery, Medical Faculty, Heinrich-Heine-University Düsseldorf, Düsseldorf, Germany

<sup>8</sup>Department of Rheumatology and Hiller Research Institute, Medical Faculty, Heinrich-Heine-University Düsseldorf, Düsseldorf, Germany

<sup>9</sup>Department of Internal Medicine I and Clinical Chemistry, University Hospital Heidelberg, Heidelberg, Germany

<sup>10</sup>Institute for Diabetes and Cancer (IDC) and Joint Heidelberg-IDC Translational Diabetes Program, Helmholtz Center Munich, Neuherberg, Germany

\*These authors contributed equally

§These authors contributed equally

§Lead contact for correspondence:

Cesare Granata, Ph. D.

Institute for Clinical Diabetology

German Diabetes Center

Auf'm Hennekamp 65

40225 Düsseldorf

Germany

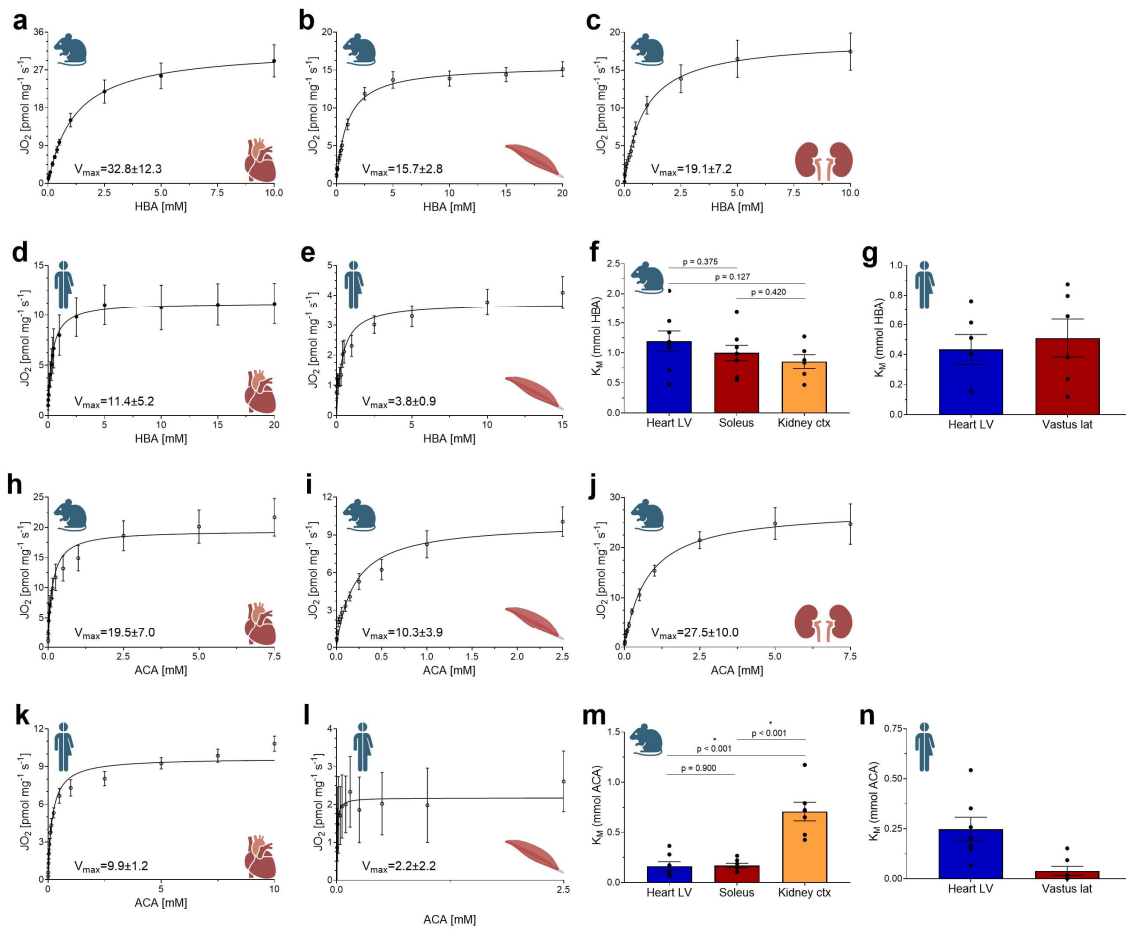
E-mail: Cesare.Granata@ddz.de

Tel.: +49 211 3382 229

## **Supplemental Material Table of Content**

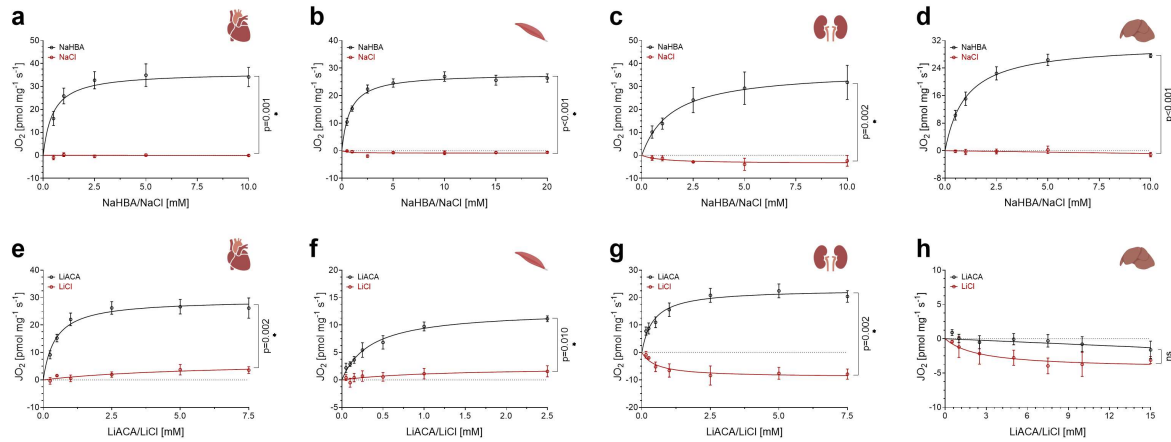
Supplementary Figure S1 – Page 3
Supplementary Figure S2 – Page 4
Supplementary Figure S3 – Page 5
Supplementary Figure S4 – Page 6
Supplementary Figure S5 – Page 7
Supplementary Figure S6 – Page 8
Supplementary Figure S7 – Page 9
Supplementary Figure S8 – Page 10
Supplementary Figure S9 – Page 11
Supplementary Figure S10 – Page 12
Supplementary Figure S11 – Page 13
Supplementary Figure S12 – Page 14
Supplementary Figure S13 – Page 15
Supplementary Figure S14 – Page 16
Supplementary Figure S15 – Page 17
Supplementary Figure S16 – Page 18
Supplementary Figure S17 – Page 19
Supplementary Table S1 – Page 20
Supplementary Table S2 – Page 21
Supplementary Table S3 – Page 22
Supplementary Table S4 – Page 23
Supplementary Table S5 – Page 24
Supplementary Table S6 – Page 25
Supplementary Table S7 – Page 26
Supplementary Table S8 – Page 27
Supplementary Table S9 – Page 28
Supplementary Table S10 – Page 29

**Supplementary Figure S1.** Michaelis-Menten kinetics for  $\beta$ -hydroxybutyrate (HBA) and acetoacetate (ACA) supported mitochondrial respiration in different mouse and human organs



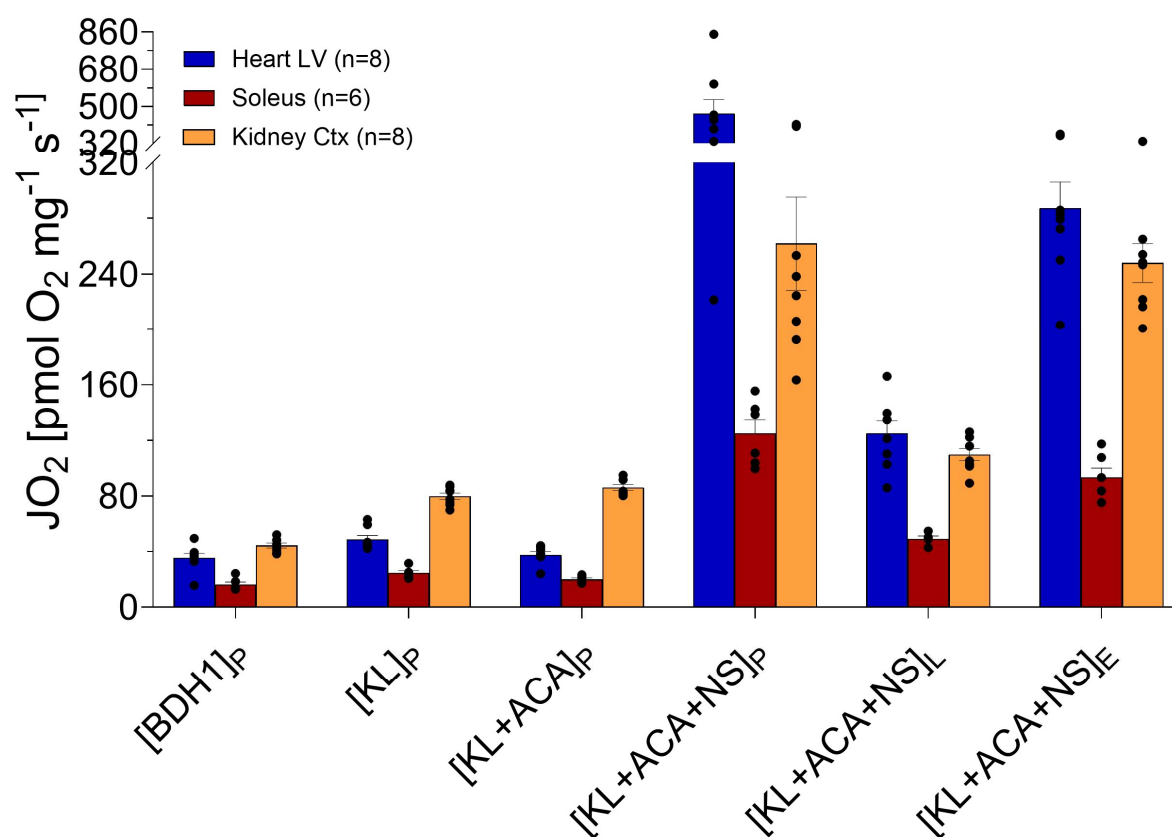
Titration of  $\beta$ -hydroxybutyrate (HBA) for mouse a) heart left ventricle, b) skeletal muscle (soleus), and c) kidney cortex, as well as human d) heart left ventricle and e) skeletal muscle (vastus lateralis), with non-linear regression fits based on the mean values according to the Michaelis-Menten Equation. The Michaelis-Menten constant ( $K_m$ ) values for each individual sample are plotted in f (mice) and g (humans), are presented as mean  $\pm$  SEM, and were compared in mice, but not humans (as the tissues were collected from different populations), using Welch's ANOVA test (panel f and m). Maximal mitochondrial respiration ( $V_{max}$ ) values are presented within each relevant panel and are expressed as [pmol  $O_2$   $mg^{-1}$   $s^{-1}$ ].  $n=6-8$  for mice.  $n=6-7$  for humans. Panels h-n represent the same analyses as a to g, respectively, following titrations with acetoacetate (ACA). For statistical reasons (i.e., calculation of  $K_m$  values in GraphPad Prism), the maximum KB concentration shown in all titration panels is the one inducing maximal  $JO_2$ , despite titrations continued up to 20-60 mM HBA and 15-30 mM ACA, depending on tissue and species, as reported in the Methods. Ctx: cortex;  $JO_2$ : oxygen flux; lat: lateralis; LV: left ventricle. Icons obtained from BioRender.com.

**Supplementary Figure S2.** Dose-response titration of sodium (NaCl) and lithium salt (LiCl) on mitochondrial respiration in different mouse organs



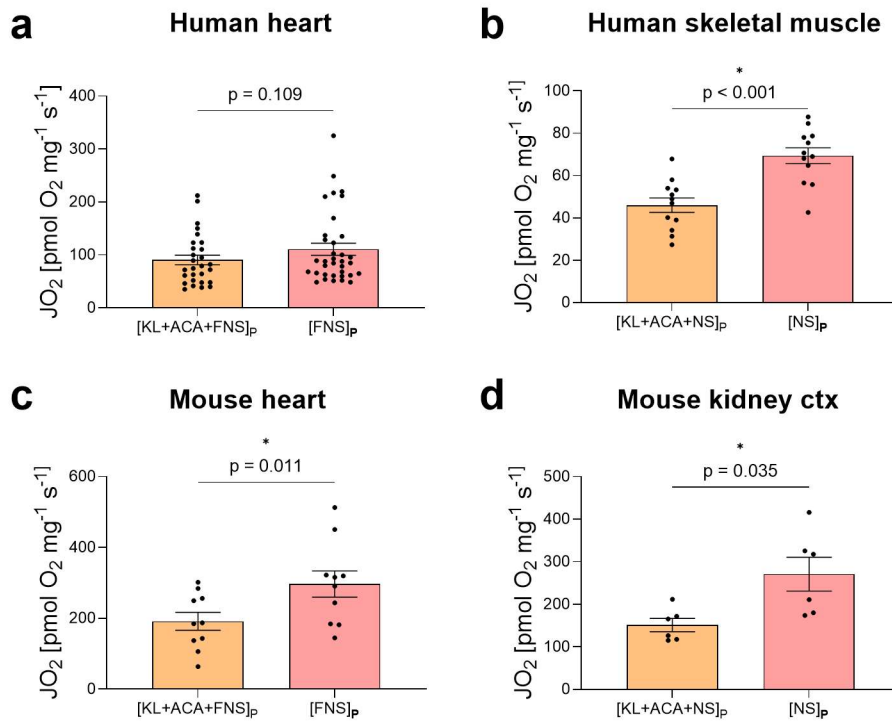
Titration of (a-d) sodium salt (NaCl) in comparison to sodium  $\beta$ -hydroxybutyrate (NaHBA) and (e-h) lithium salt (LiCl) in comparison to lithium acetoacetate (LiACA) in the mouse (a, e) heart left ventricle, (b, f) skeletal muscle (soleus), (c, g) kidney cortex, and (d, h) liver. Mitochondrial respiration is expressed as [pmol O<sub>2</sub> mg<sup>-1</sup> s<sup>-1</sup>] and mean  $\pm$  SEM. n=3 for NaHBA vs. NaCl. n=3 for LiACA vs. LiCl. The data were fitted using non-linear regression and differences between groups were determined using a repeated-measurements mixed-effects model.<sup>1</sup> For statistical reasons (i.e., calculation of K<sub>m</sub> values in GraphPad Prism), the maximum KB concentration shown in all titration panels is the one inducing maximal JO<sub>2</sub>, despite titrations continued up to 20-60 mM HBA and 15-30 mM ACA, depending on tissue and species, as reported in the Methods. n=3. JO<sub>2</sub>: oxygen flux. Icons obtained from BioRender.com.

**Supplementary Figure S3.** Full KB protocol including standard substrates in various mouse organs



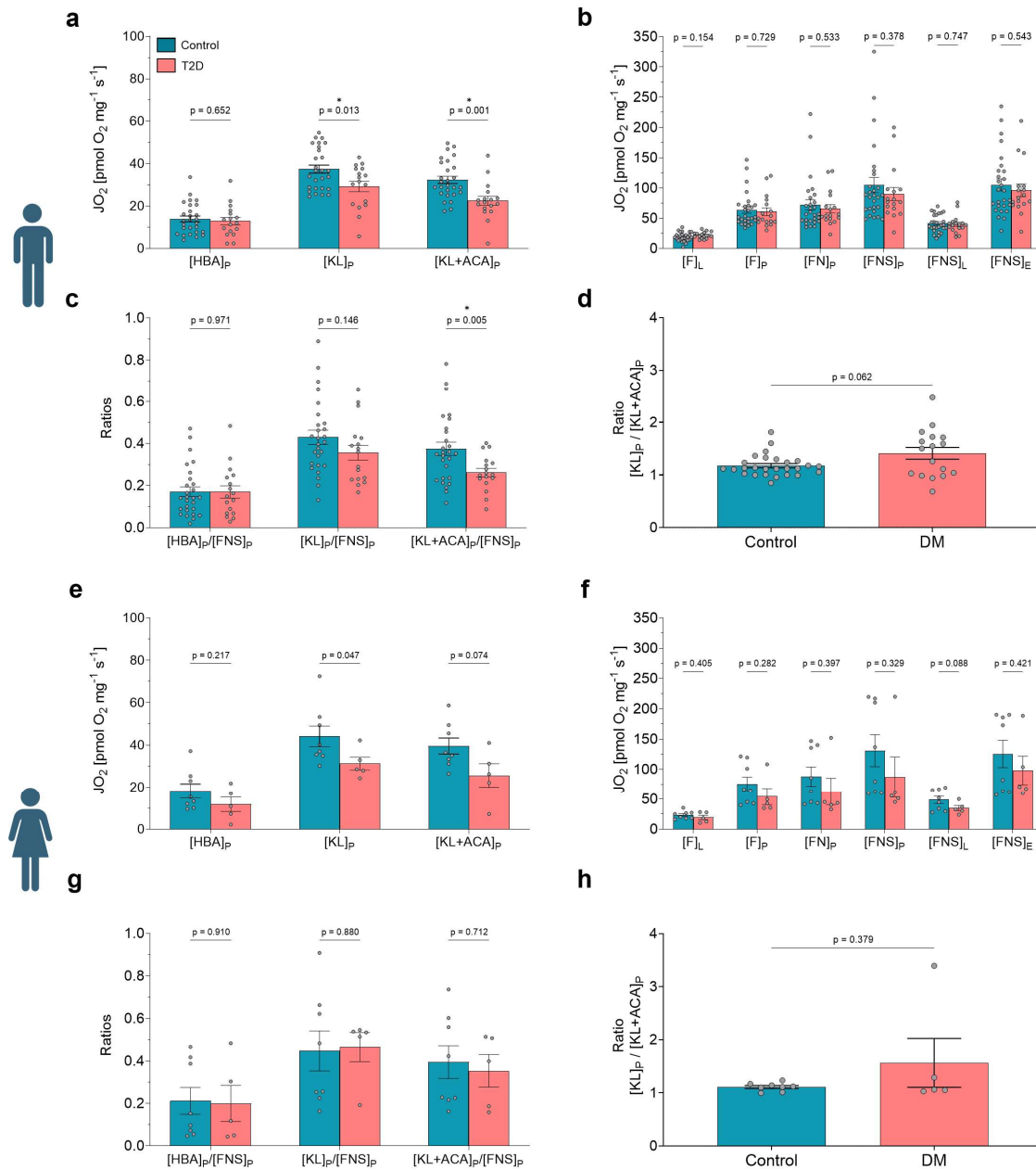
Substrate-Uncoupler-Inhibitor Titration (SUIT) protocol in mouse heart left ventricle (LV), skeletal muscle (soleus), and kidney cortex; data are mean  $\pm$  SEM. No statistical hypothesis testing was performed. ACA: acetoacetate; BDH1:  $\beta$ -hydroxybutyrate dehydrogenase; <sub>E</sub>: electron transport chain capacity (noncoupled) mitochondrial respiration state;  $JO_2$ : oxygen flux; <sub>L</sub>: leak mitochondrial respiration state; KL: ketolysis; N: NADH-linked substrates; <sub>p</sub>: phosphorylating (coupled) mitochondrial respiration state; S: succinate-linked substrates.

**Supplementary Figure S4.** Comparison between prior addition of ketone body metabolism substrates versus no addition



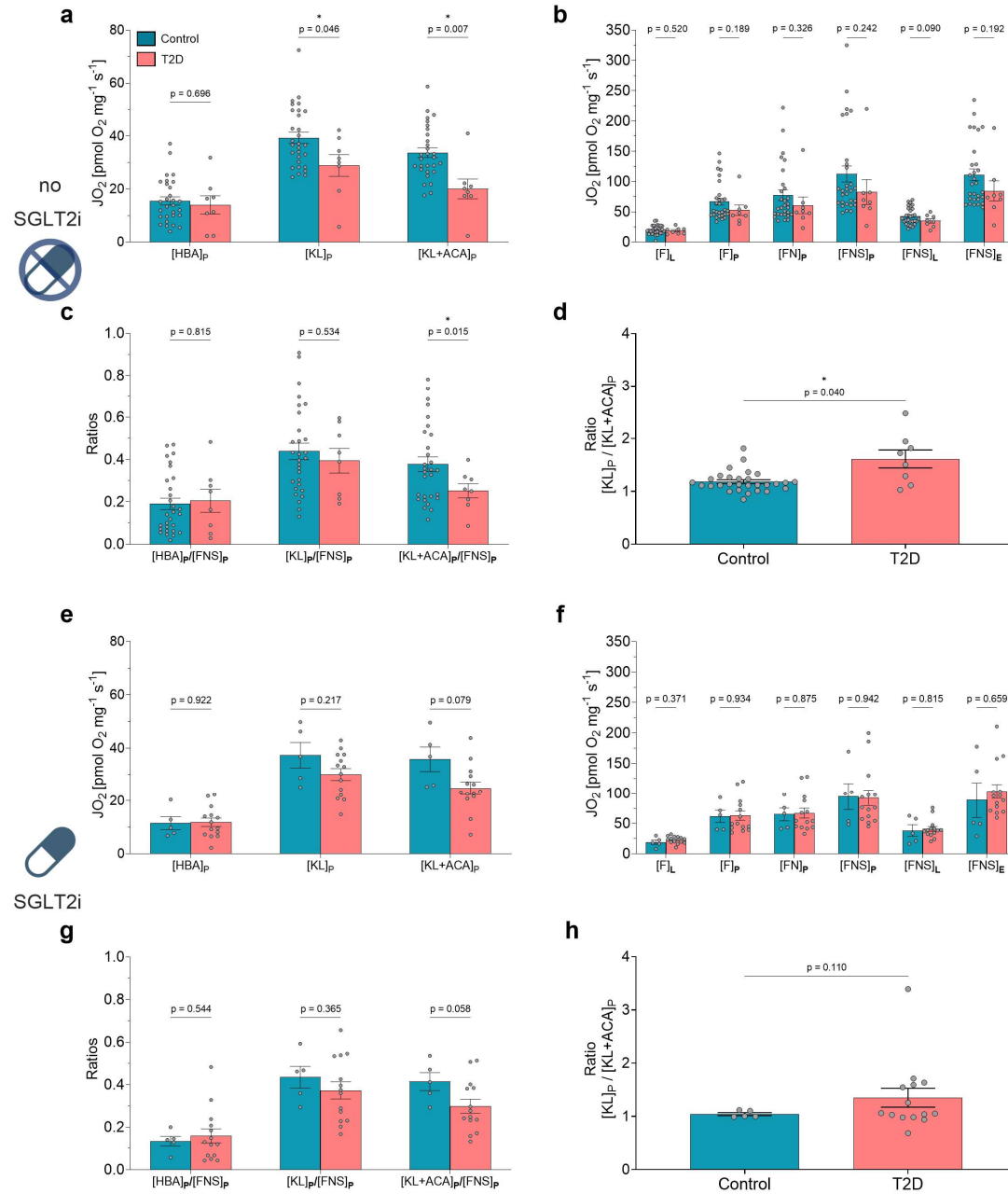
Maximal oxidative phosphorylation (OXPHOS) capacity with (KL+ACA+FNS<sub>P</sub>, or KL+ACA+NS<sub>P</sub>) and without (FNS<sub>P</sub>, or NS<sub>P</sub>) addition of ketone bodies in permeabilized (a) ventricular myocardium (KL+ACA+FNS<sub>P</sub>: n=28, FNS<sub>P</sub>: n=35), (b) human skeletal muscle (vastus lateralis; n=12), (c) mouse heart left ventricle (n=10), and (d) mouse kidney cortex (n=6) from the control groups utilized for generation of Figure 2, 3, 2, and 4, respectively. Data are mean ± SEM. Wilcoxon signed-rank test (a) or paired t-test (b-d). ACA: acetoacetate; F: fatty acid oxidation-linked substrates; JO<sub>2</sub>: oxygen flux; KL: ketolysis; N: NADH-linked substrates; P: phosphorylating (coupled) mitochondrial respiration state; S: succinate-linked substrates.

## Supplementary Figure S5. Ketone body dependent OXPHOS capacity in male and female human diabetic heart



Mitochondrial respiration (JO<sub>2</sub>) of permeabilised ventricular myocardium of heart transplant recipients undergoing routine endomyocardial biopsy from males (a-d) and females (e-h) without (Control) versus with Type 2 Diabetes (T2D), obtained with (a and e) the combined ketone body (KB) and (b and f) the fatty acid oxidation (F), NADH (N), and succinate (S) combined (FNS) pathway mitochondrial respiration protocols. (c and g) Relative contribution of the different respiratory states of KB-linked versus maximal coupled FNS-linked mitochondrial respiration. (d and h) [KL]<sub>p</sub>/[KL+ACA]<sub>p</sub> ratio. a-c and e-f: repeated-measurements mixed-effects model (REML) with correction for multiple testing with the false discovery rate.<sup>1</sup> d and h: Welch's t-test. Males n=27 (Control) vs. 17 (T2D). Females n=8 (Control) vs. 5 (T2D). Data are mean ± SEM. HBA: β-hydroxybutyrate; KL: ketolysis; L: leak mitochondrial respiration state; p: phosphorylating (coupled) mitochondrial respiration state; E: electron transport chain capacity (noncoupled) mitochondrial respiration state; JO<sub>2</sub>: oxygen flux. Icons obtained from BioRender.com.

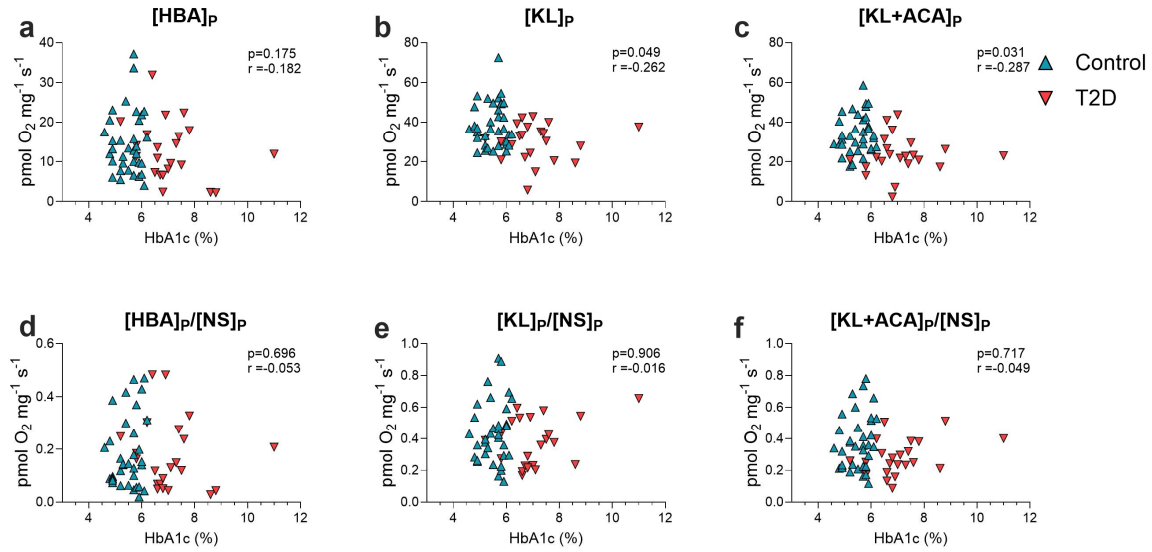
## Supplementary Figure S6. Ketone body dependent OXPHOS capacity in the human diabetic heart with and without SGLT2 inhibitor therapy



Mitochondrial respiration ( $JO_2$ ) in permeabilised ventricular myocardium of heart transplant recipients undergoing routine endomyocardial biopsy without (Control) versus with Type 2 Diabetes (T2D) and without (a-d) and with (e-h) sodium-glucose-cotransporter 2 inhibitor (SGLT2i) therapy. Data were obtained with the (a, e) combined KB protocol and (b, f) the fatty acid oxidation (F), NADH (N), and succinate (S) combined (FNS) pathway mitochondrial respiration protocols. (c, g) Relative contribution of the different respiratory states of KB-linked versus maximal coupled FNS-linked mitochondrial respiration. (d, h)  $[KL]_P/[KL+ACA]_P$  ratio. No SGLT2i: n=29 (Control) vs. 8 (T2D). SGLT2i therapy: n=5 (Control) vs. n=14 (T2D). Data are mean  $\pm$  SEM. a-c, e-g: repeated-measurements mixed-effects (REML) model with correction for multiple testing with the false discovery rate.<sup>1</sup> d, h: Welch's t-test. ACA: acetoacetate; HBA:  $\beta$ -hydroxybutyrate;  $JO_2$ : oxygen flux; KL: ketolysis; <sub>P</sub>: phosphorylating (coupled) mitochondrial respiration state; Icons obtained from BioRender.com.

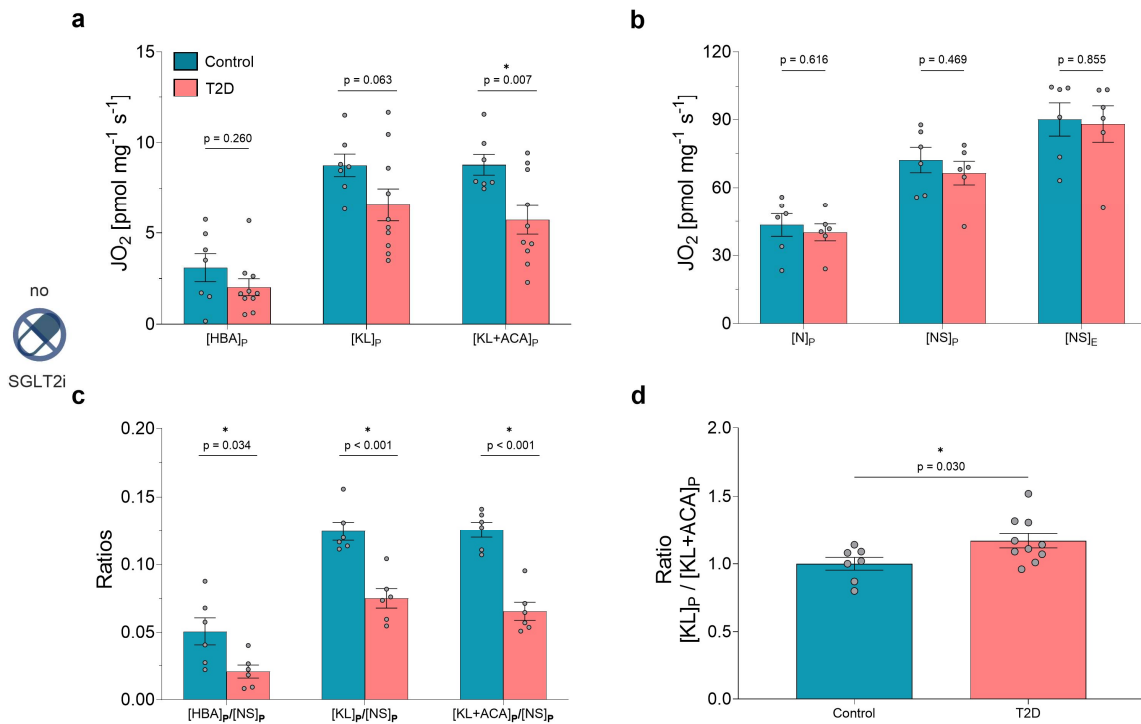


**Supplementary Figure S7.** Correlations between haemoglobin A1<sub>c</sub> and ketone body-linked oxidative phosphorylation (OXPHOS) capacity in human myocardium



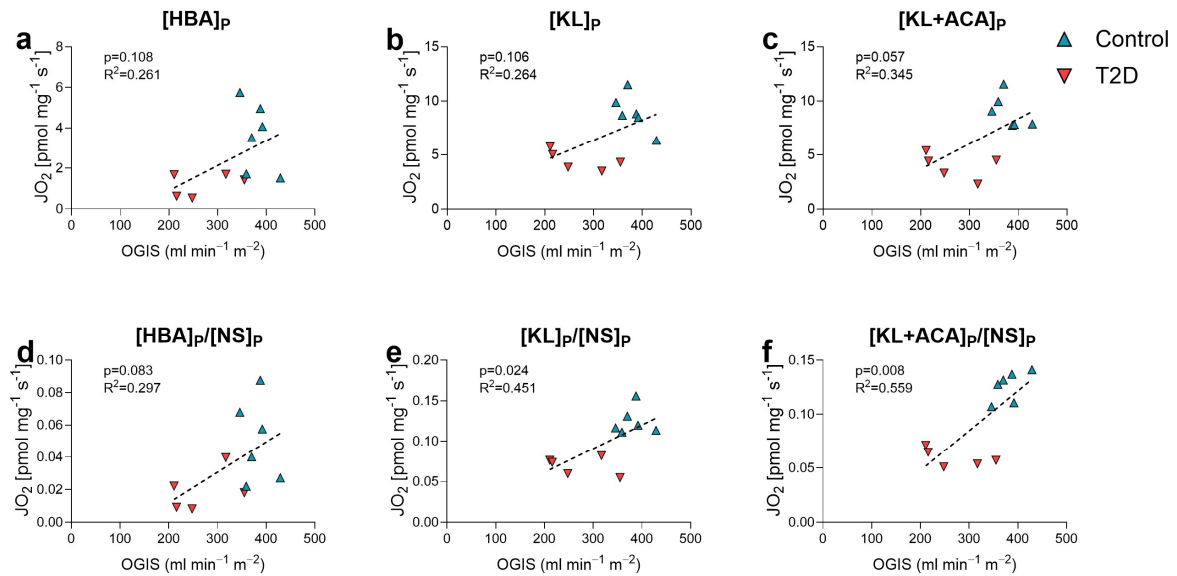
Spearman correlation was used to assess the association of haemoglobin A1<sub>c</sub> (HbA1<sub>c</sub>) and different KB respiratory states in human myocardium: a) [BDH1]<sub>P</sub>, b) [KL]<sub>P</sub>, c) [KL+ACA]<sub>P</sub>, d) [BDH1]<sub>P</sub>/[NS]<sub>P</sub>, e) [KL]<sub>P</sub>/[NS]<sub>P</sub>, f) [KL+ACA]<sub>P</sub>/[NS]<sub>P</sub>. n=22 (T2D) and n=35 (Control). ACA: acetoacetate; BDH1: β-hydroxybutyrate dehydrogenase; KL: ketolysis; N: NADH-linked substrates; P: phosphorylating (coupled) mitochondrial respiration state; S: succinate-linked substrates.

**Supplementary Figure S8.** Ketone body dependent OXPHOS capacity in the type 2-diabetic skeletal muscle without SGLT2 inhibitor therapy



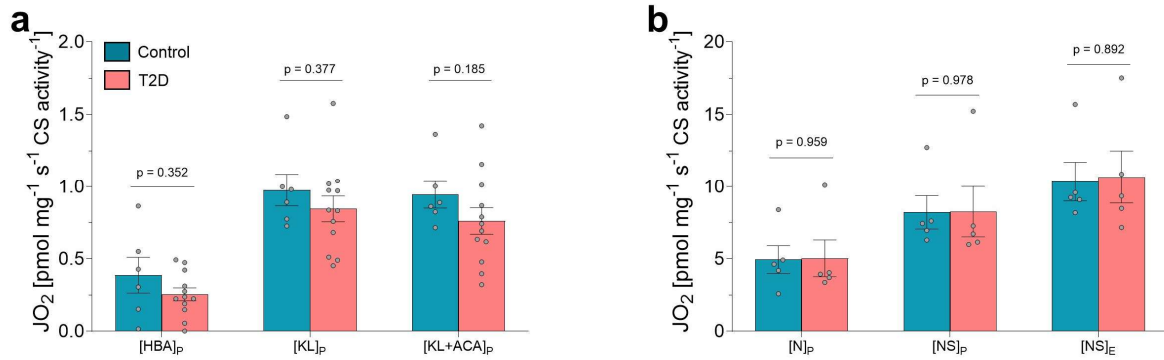
Mitochondrial respiration ( $JO_2$ ) in permeabilised skeletal muscle (vastus lateralis) fibres from type 2 diabetes (T2D) versus glucose-tolerant (Control) individuals not taking any sodium-glucose-cotransporter 2 inhibitors (SGLT2i), obtained with the (a) combined KB protocol and (b) the NADH (N) and succinate (S) combined (NS) pathway mitochondrial respiration protocols. (c) Relative contribution of the different respiratory states of KB-linked versus maximal coupled NS-linked mitochondrial respiration. (d)  $[KL]_p/[KL+ACA]_p$  ratio. a, d: n=7 vs. 10. b, c: n=6 vs. 6. Data are mean  $\pm$  SEM. a-c: repeated-measurements mixed-effects (REML) model with correction for multiple testing with the false discovery rate.<sup>1</sup> d: Welch's t-test. ACA: acetoacetate; HBA:  $\beta$ -hydroxybutyrate;  $JO_2$ : oxygen flux; KL: ketolysis; <sub>p</sub>: phosphorylating (coupled) mitochondrial respiration state; Icons obtained from BioRender.com.

**Supplementary Figure S9.** Correlations between insulin sensitivity and ketone body-linked oxidative phosphorylation (OXPHOS) capacity in human skeletal muscle



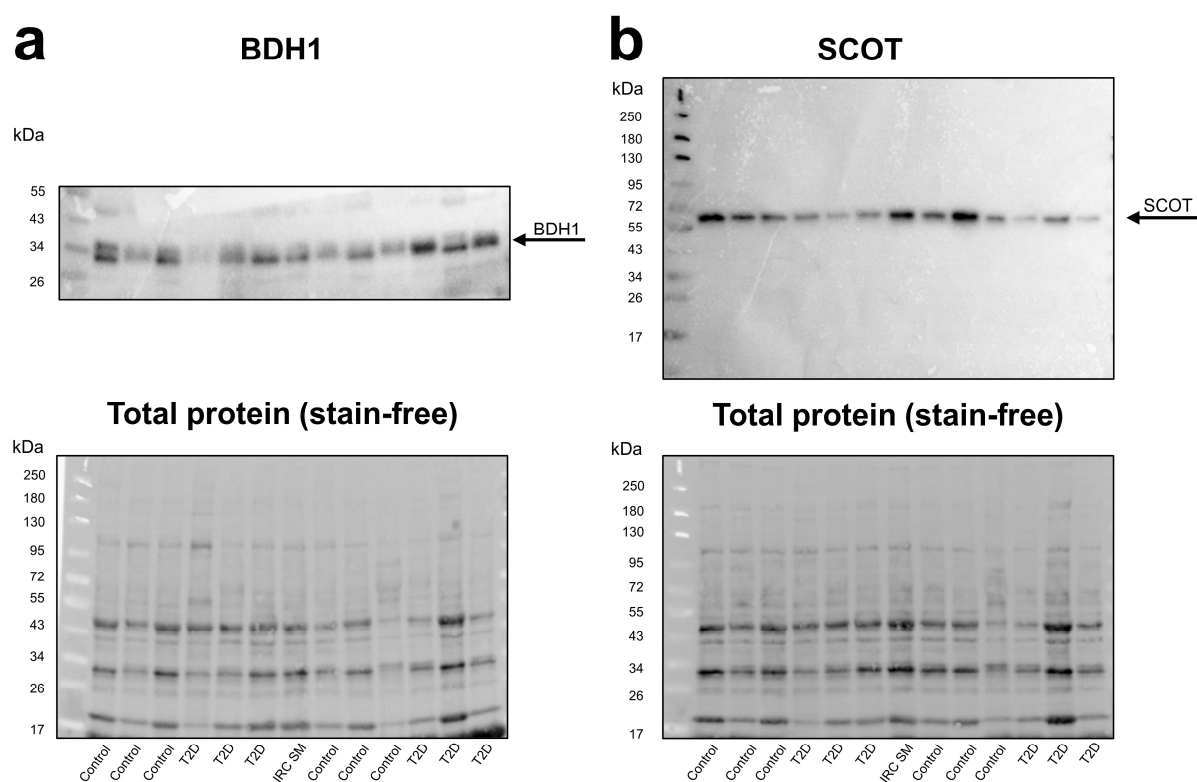
Univariate linear regression models were used to assess the association of oral glucose insulin sensitivity (OGIS) index and different KB respiratory states in human skeletal muscle: a) [BDH1]<sub>P</sub>, b) [KL]<sub>P</sub>, c) [KL+ACA]<sub>P</sub>, d) [BDH1]<sub>P</sub>/[NS]<sub>P</sub>, e) [KL]<sub>P</sub>/[NS]<sub>P</sub>, f) [KL+ACA]<sub>P</sub>/[NS]<sub>P</sub>. n=5 (T2D) and 6 (Control). ACA: acetoacetate; BDH1:  $\beta$ -hydroxybutyrate dehydrogenase; KL: ketolysis; N: NADH-linked substrates; <sub>P</sub>: phosphorylating (coupled) mitochondrial respiration state; <sub>S</sub>: succinate-linked substrates.

**Supplementary Figure S10.** Oxidative phosphorylation (OXPHOS) capacity in the type 2-diabetic skeletal muscle normalized for mitochondrial content



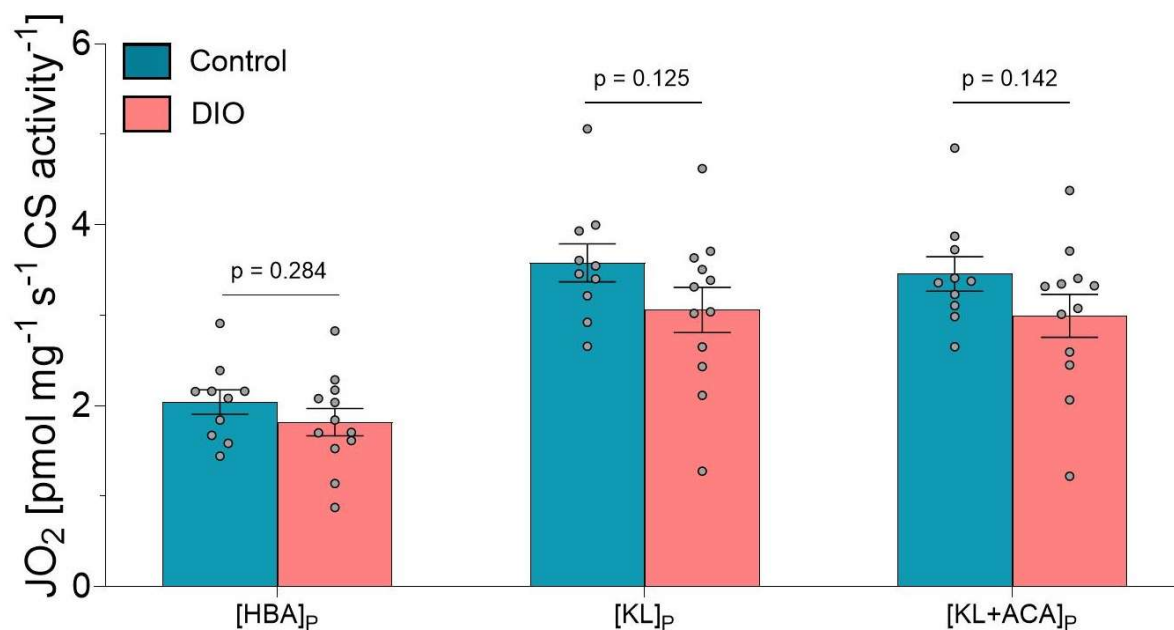
Mitochondrial respiration ( $\text{JO}_2$ ) normalized for Citrate Synthase (CS) activity in permeabilised skeletal muscle (vastus lateralis) fibres from type 2 diabetes (T2D) versus glucose-tolerant (Control) individuals using the (a) combined ketone body (KB) and (b) the combined NADH (N) and succinate (S) pathway (NS) mitochondrial respiration protocol.  $n=6$  vs.  $n=12$  (a, KB SUI),  $n=5$  vs.  $n=5$  (b, NS SUI). Repeated measurement mixed-effects (REML) model with correction for multiple testing with the false discovery rate.<sup>1</sup> Data are presented as mean  $\pm$  SEM. ACA: acetoacetate; HBA:  $\beta$ -hydroxybutyrate;  $\epsilon$ : electron transport chain capacity (noncoupled) mitochondrial respiration state;  $\text{JO}_2$ : oxygen flux; KL: ketolysis; P: phosphorylating (coupled) mitochondrial respiration state.

**Supplementary Figure S11.** Immunoblot of  $\beta$ -hydroxybutyrate dehydrogenase (BDH1) and succinyl-CoA: 3-ketoacid (oxoacid) coenzyme A transferase (SCOT) protein expression in the type 2-diabetic skeletal muscle



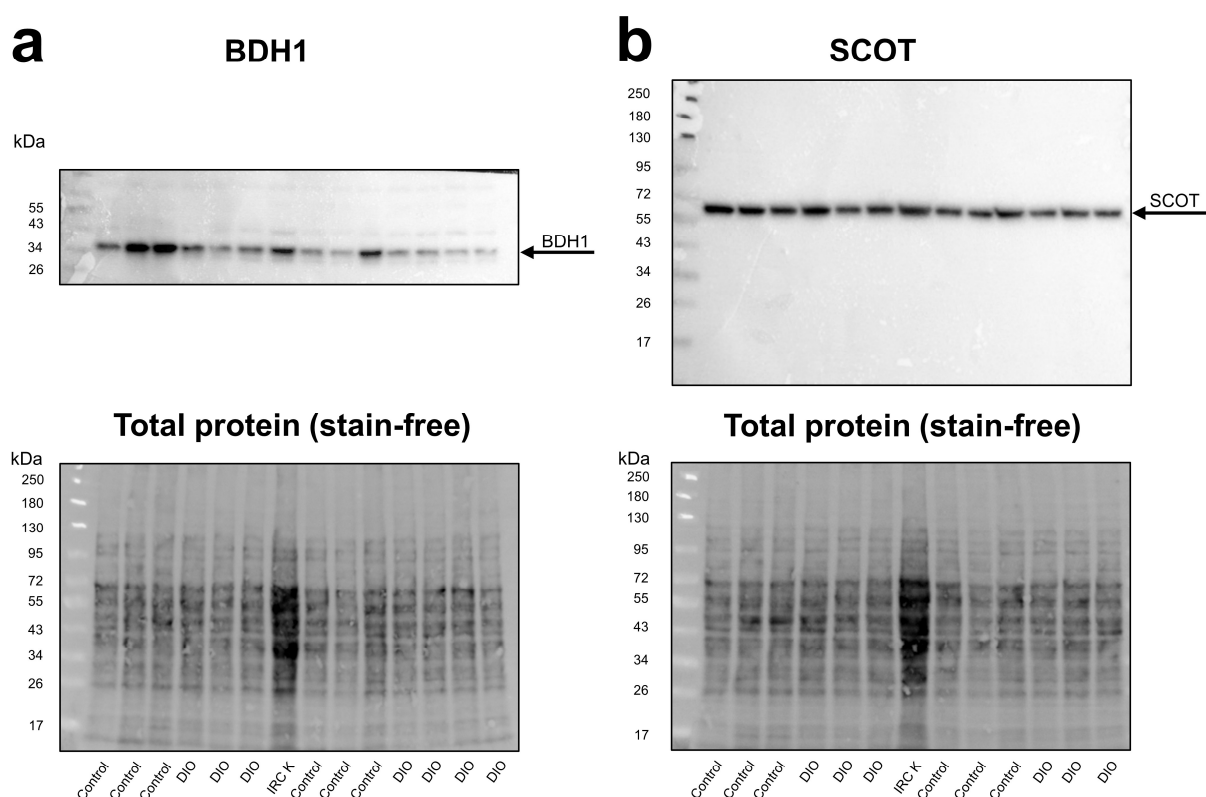
Expression of the ketolytic enzymes (a) BDH1 and (b) SCOT was measured in skeletal muscle (vastus lateralis) fibres from type 2 diabetes (T2D) versus glucose-tolerant (Control) individuals. Unprocessed, representative immunoblots of BDH1 and SCOT protein expression, as well as total protein membrane stain-free images are shown for 6 Controls and 6 T2D individuals. For imaging of BDH1, membranes were cut below 26 kDa and above 55 kDa, to improve the signal to noise ratio. Protein expression was normalized to the total protein content of the same membrane measured using stain-free images. For analysis and comparison of samples on different gels, an inter-run calibrator skeletal muscle sample (IRC SM) was loaded on each gel as a reference sample to correct for gel-to-gel variation.<sup>2</sup> The sources and catalogue numbers of the respective antibodies are provided in Supplementary Table S3.

**Supplementary Figure S12.** Oxidative phosphorylation (OXPHOS) capacity in the kidney cortex of diet induced obesity (DIO) male mice normalized for mitochondrial content



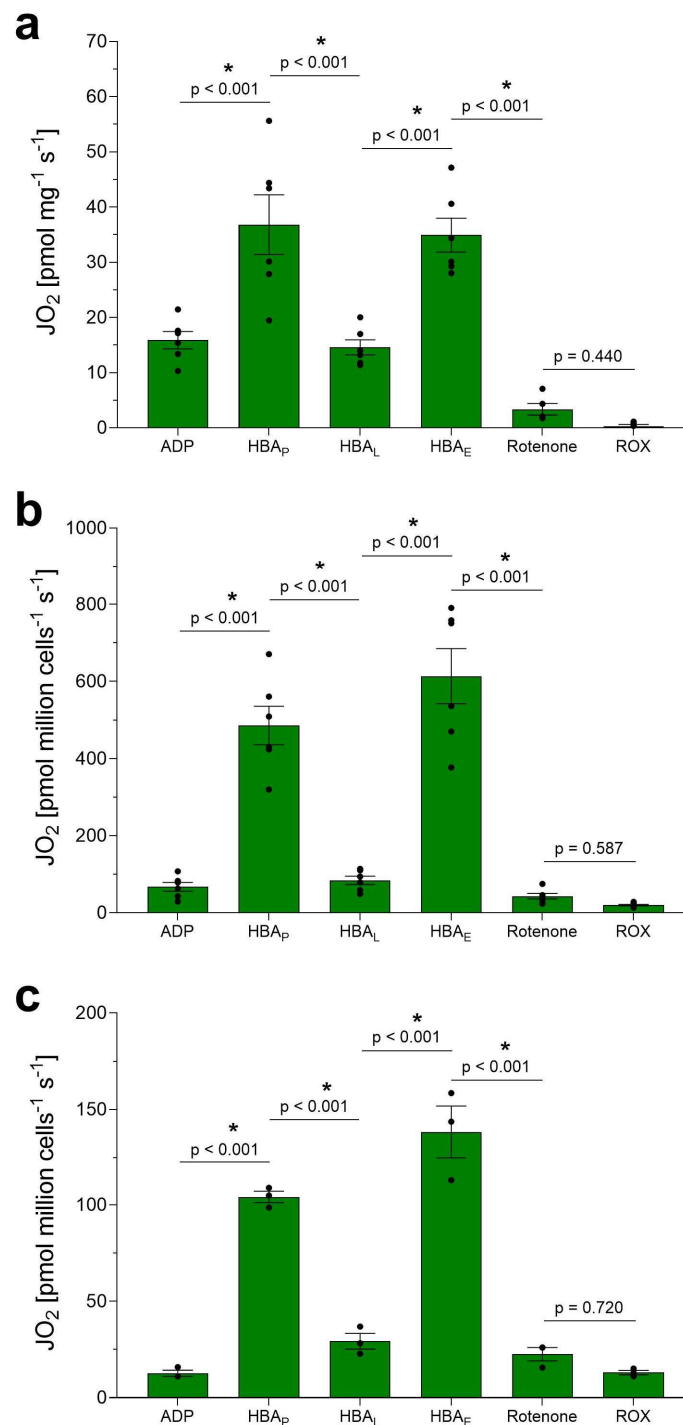
Mitochondrial respiration ( $JO_2$ ) normalized for Citrate Synthase (CS) activity in the permeabilised kidney cortex from diet-induced obese (DIO) versus normal chow diet-fed (Control) C57BL/6J male mice obtained with the combined ketone body mitochondrial respiration protocol.  $n = 10$  vs.  $12$ . Repeated measurement mixed-effects (REML) model with correction for multiple testing with the false discovery rate.<sup>1</sup> Data are presented as mean  $\pm$  SEM. ACA: acetoacetate; HBA:  $\beta$ -hydroxybutyrate;  $JO_2$ : oxygen flux; KL: ketolysis;  $P$ : phosphorylating (coupled) mitochondrial respiration state.

**Supplementary Figure S13.** Immunoblot of  $\beta$ -hydroxybutyrate dehydrogenase (BDH1) and succinyl-CoA: 3-ketoacid (oxoacid) coenzyme A transferase (SCOT) protein expression in the kidney cortex of diet induced obesity (DIO) male mice



Expression of the ketolytic enzymes (a) BDH1 and (b) SCOT was measured in kidney cortex from diet induced obese (DIO) versus normal chow diet-fed (Control) C57BL/6J male mice. Unprocessed, representative immunoblots of BDH1 and SCOT protein expression, as well as total protein membrane stain-free images are shown for 6 Controls and 7 (BDH1) or 6 (SCOT) DIO mice. For imaging of BDH1, membranes were cut below 26 kDa and above 55 kDa to improve the signal to noise ratio. Protein expression was normalized to the total protein content of the same membrane measured using stain-free images. For analysis and comparison of samples on different gels, an inter-run calibrator kidney sample (IRC K) was loaded on each gel as reference sample to correct for gel-to-gel variation.<sup>2</sup> The sources and catalogue numbers of the respective antibodies are provided in Supplementary Table S3.

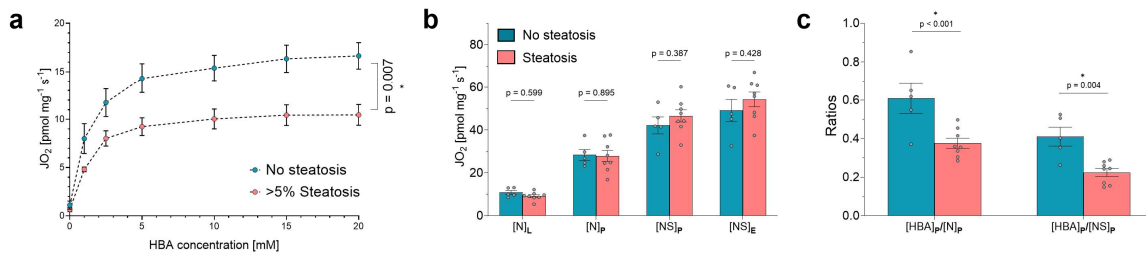
**Supplementary Figure S14.** HBA-driven O<sub>2</sub> consumption in mouse liver stems from generation of ATP by the ETS



Substrate-Uncoupler-Inhibitor Titration (SUIT) protocol in (a) mouse liver, (b) mouse and (c) human primary hepatocytes (substrates added in the presence of ADP). a-b: n=6, c: n=3. Data are expressed as mean  $\pm$  SEM. Repeated-measurements mixed-effects model (REML) with correction for multiple testing with the false discovery rate (1). ADP: adenosine diphosphate;  $\epsilon$ : electron transport chain capacity (noncoupled) mitochondrial respiration state; HBA:  $\beta$ -hydroxybutyrate; JO<sub>2</sub>: oxygen flux;  $\text{L}$ : leak mitochondrial respiration state;  $\text{p}$ : phosphorylating (coupled) mitochondrial respiration state; ROX: residual oxygen consumption.

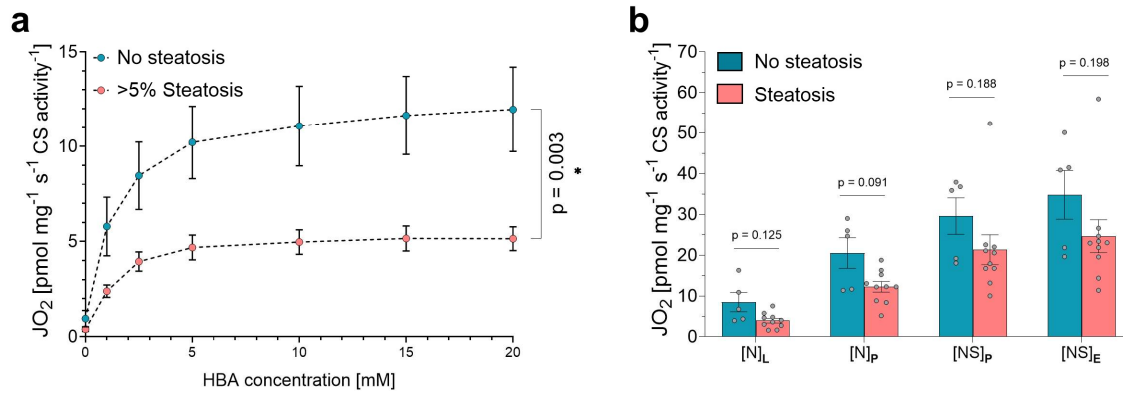


**Supplementary Figure S15.** Hepatic  $\beta$ -hydroxybutyrate (HBA)-supported mitochondrial OXPHOS capacity in female human individuals with steatosis



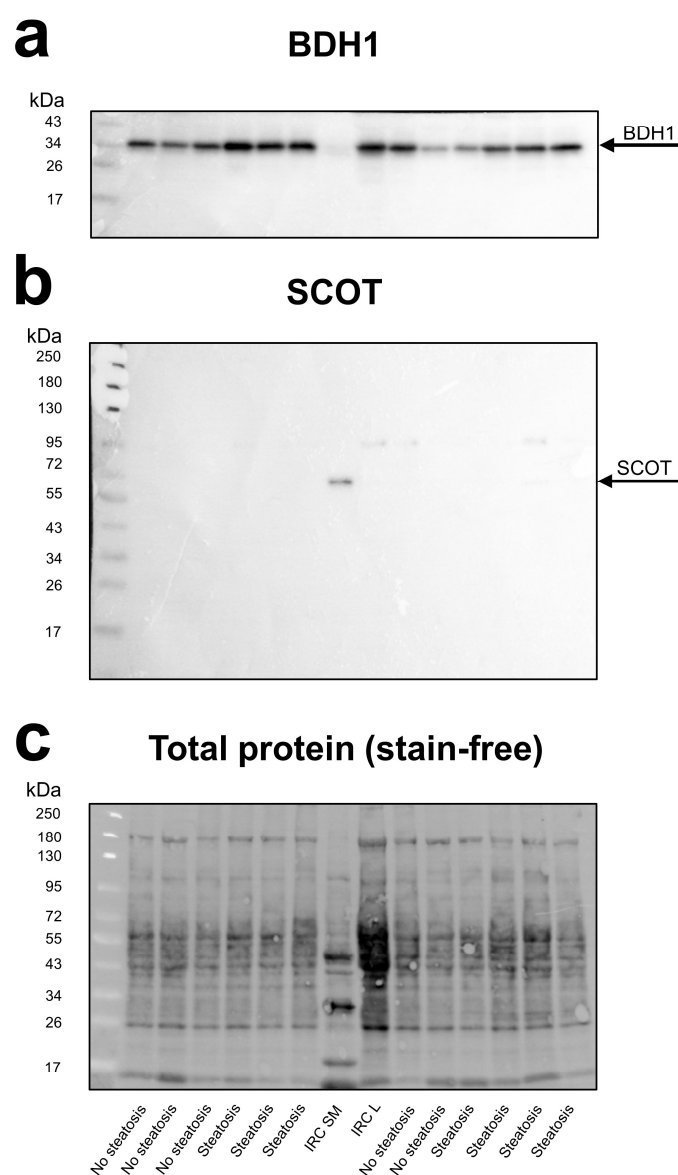
Mitochondrial respiration (JO<sub>2</sub>) in human whole-liver from female participants with and without hepatic steatosis (cut off: histological hepatic fat content >5%), obtained with (a) HBA titrations (0, 1, 2.5, 5, 10, 15, 20 mM of HBA) in the presence of saturating levels of ADP and (b) the NADH (N) and succinate (S) combined (NS) pathway mitochondrial respiration protocol. (c) Relative contribution of the [HBA]<sub>p</sub> respiratory state versus the maximal coupled N- and NS-linked mitochondrial respiration states. n=5 (No steatosis) vs. 8 (Steatosis). a: Non-linear regression curves were fitted to the data points and differences between groups were determined using repeated-measurements ANOVA. b, c: repeated-measurements mixed-effects model (REML) with correction for multiple testing with the false discovery rate<sup>1</sup>. Data are mean ± SEM. For statistical reasons (i.e., calculation of K<sub>m</sub> values in GraphPad Prism), the maximum KB concentration shown in all titration panels is the one inducing maximal JO<sub>2</sub>, despite titrations continued up to 20–60 mM HBA and 15–30 mM ACA, depending on tissue and species, as reported in the Methods. E: electron transport chain capacity (noncoupled) mitochondrial respiration state; JO<sub>2</sub>: oxygen flux; L: leak mitochondrial respiration state; p: phosphorylating (coupled) mitochondrial respiration state.

**Supplementary Figure S16.** Hepatic oxidative phosphorylation (OXPHOS) capacity in individuals with steatosis normalized for mitochondrial content



(a)  $JO_2$  values from the titration of  $\beta$ -hydroxybutyrate (HBA) in the presence of saturating levels of ADP normalized for Citrate Synthase (CS) activity in human whole-liver from participants with and without hepatic steatosis (cut-off: histological hepatic fat content >5%). HBA titration steps: 0, 1, 2.5, 5, 10, 15, 20 mM of HBA. (b)  $JO_2$  values from the NADH (N) and succinate (S) combined (NS) pathway mitochondrial respiration protocol normalized for Citrate Synthase (CS) activity.  $n = 5$  (No Steatosis) vs. 11 (Steatosis). a: non-linear regression curves were fitted to the data points and differences between groups were determined using repeated-measurements ANOVA.<sup>(1)</sup> b: repeated-measurements mixed-effects (REML) models with correction for multiple testing with the false discovery rate.<sup>1</sup> Data are presented as mean  $\pm$  SEM. E: electron transport chain capacity (noncoupled) mitochondrial respiration state;  $JO_2$ : oxygen flux; L: leak mitochondrial respiration state; P: phosphorylating (coupled) mitochondrial respiration state.

**Supplementary Figure S17.** Immunoblot of  $\beta$ -hydroxybutyrate dehydrogenase (BDH1) and succinyl-CoA: 3-ketoacid (oxoacid) coenzyme A transferase (SCOT) protein expression in the human steatotic liver



Expression of the ketolytic enzymes (a) BDH1 and (b) SCOT in the liver of individuals with and without steatosis. Unprocessed, representative immunoblots of BDH1 and SCOT protein expression as well as total protein staining are shown for 5 individuals without and 7 individuals with steatosis. For imaging of BDH1, membranes were cut below 26 kDa and above 55 kDa, to improve the signal to noise ratio. Protein expression was normalized to the total protein content of the same membrane measured using stain-free images. Because SCOT is not expressed in liver tissue, a positive control (inter-run calibrator for skeletal muscle [IRC SM]) was loaded on each gel to validate the ability of the anti-SCOT antibody to detect SCOT. For analysis and comparison of samples on different gels, an inter-run calibrator liver sample (IRC L), which also acted as negative control, was loaded on each gel as reference sample to correct for gel-to-gel variation.<sup>2</sup> The sources and catalogue numbers of the respective antibodies are provided in Supplementary Table S3.

**Supplementary Table S1.** Combined KB Substrate-Uncoupler-Inhibitor-Titration (SUIT) respirometry protocols in mice

Agent	Organ			
	Myocardium	Skeletal Muscle (soleus)	Kidney Cortex	Liver
Saponin	50 µg/ml	50 µg/ml	100 µg/ml	-
Sample (mg per chamber)	~1.0-1.2 mg	~1.3-1.8 mg	~0.9-1.3 mg	~1.7-2.2 mg
Oxygen	~480 µmol	~480 µmol	~480 µmol	~480 µmol
ADP	5 mM	5 mM	5 mM	5 mM
DL-β-hydroxybutyrate	10 mM	20 mM	10 mM	10 mM
Malate	2 mM	2 mM	2 mM	-
Acetoacetate (single injection)	1 mM	1 mM	1 mM	-
Octanoyl-L-Carnitine	1 mM	-	-	-
Pyruvate	5 mM <sup>#</sup>	5 mM	5 mM	-
Glutamate	10 mM	10 mM	10 mM	-
Succinate	10 mM	10 mM	10 mM	-
Oligomycin	2.5 µM	2.5 µM	2.5 µM	2.5 µM
FCCP	1-2 µl steps (0.75-1.5 µM)	1-2 µl steps (0.75-1.5 µM)	1-2 µl steps (0.75-1.5 µM)	1-2 µl steps (0.75-1.5 µM)
Rotenone	-	-	-	0.5 µM
Antimycin A	5 µM	5 µM	5 µM	5 µM
Mitochondrial respiration of the left ventricle, kidney cortex, soleus muscle, and liver was evaluated using the Oxygraph-2k (Oroboros Instruments, Innsbruck, Austria) at 37°C, an active chamber volume of 2 mL, and a stirrer speed of 750 rpm acquiring every 2 sec. The SUIT protocol can be performed in the order and final concentrations indicated, and/or can be modified ad hoc. The HBA and ACA concentrations used are based on preliminary titrations. Depending on the species or pathologies, different concentrations of HBA and ACA may be required. <sup>#</sup> Pyruvate was not added in the analysis of permeabilized myocardium in figure 2.				

FCCP: carbonyl cyanide-p-trifluoromethoxyphenylhydrazone.

**Supplementary Table S2.** Combined KB Substrate-Uncoupler-Inhibitor-Titration (SUIT) respirometry protocols in humans

Agent	Organ		
	Myocardium	Skeletal Muscle (vastus lateralis)	Liver
Saponin	50 µg/ml	50 µg/ml	-
Sample (mg per chamber)	~1.0-1.2 mg	~2.5.3.5 mg	~2.0.2.5 mg
Oxygen	~480 µmol	~480 µmol	~480 µmol
ADP	2.5 mM	5 mM	5 mM
DL-β-hydroxybutyrate	5 mM	20 mM	Titration (in mM): 1, 2.5, 5, 10, 15, 20, 30, 40
Malate	2 mM	2 mM	-
Acetoacetate	1/5 mM	1 mM	-
Octanoyl-L-Carnitine	1.0 mM	-	-
Pyruvate	5 mM <sup>#</sup>	5 mM	-
Glutamate	10 mM	10 mM	-
Succinate	10 mM	10 mM	-
Oligomycin	5 µM	-	-
FCCP	1-2 µl steps (0.75-1.5 µM)	1-2 µl steps (0.75-1.5 µM)	-
Antimycin A	5 µM	5 µM	5 µM
Mitochondrial respiration of the left ventricle, vastus lateralis muscle and liver was assessed using the Oxygraph-2k (Oroboros Instruments, Innsbruck, Austria) at 37°C, an active chamber volume of 2 mL, and a stirrer speed of 750 rpm acquiring every 2 sec. The SUIT protocol can be performed in the order and final concentrations indicated, and/or can be modified ad hoc. The HBA and ACA concentrations used are based on preliminary titrations. Depending on the population or pathologies, different concentrations of HBA and ACA may be required. <sup>#</sup> Pyruvate was not added in the analysis of permeabilized myocardium in figure 2.			

FCCP: carbonyl cyanide-p-trifluoromethoxyphenylhydrazone.

**Supplementary Table S3.** Western blot antibody sources and catalogue numbers

<b>Antibody</b>	<b>Species</b>	<b>Organ</b>	<b>Source</b>	<b>Catalogue number</b>
Anti-OXCT1/SCOT antibody	human, mouse	skeletal muscle, kidney, liver	Abcam	ab241125
Anti-BDH1 antibody	human	liver	Abcam	ab193156
Anti-BDH1 antibody	human, mouse	skeletal muscle, kidney	Proteintech	15417-1-AP
Anti-rabbit IgG HRP-conjugated	human, mouse	skeletal muscle, kidney, liver	Cell Signaling Technology	7074

**Supplementary Table S4.** Characteristics of human participants in heart cohorts

Characteristic	Control, N = 35 <sup>1</sup>	T2D, N = 22 <sup>1</sup>	p-value <sup>2</sup>	Difference <sup>3</sup>
Age (years)	56.00 [50.00; 61.00]	62.00 [55.50; 64.25]	0.064	4.50 [0.00; 8.00]
Sex (male)	27 (77.14 %)	17 (77.27 %)	>0.999	0.13% [-22.46%; 26.07%]
BMI (kg/m <sup>2</sup> )	24.21 [21.30; 26.30]	26.58 [23.33; 30.72]	0.018	3.35 [0.52; 5.73]
HbA1c (%)	5.70 [5.20; 5.90]	6.85 [6.48; 7.53]	<0.001	1.40 [1.00; 1.80]
Free fatty acids (μmol/L)	590 [430; 1400]	1350 [862.5; 2325]	0.007	500 [200;1220]
Metformin	0 (0 %)	5 (22.73 %)	0.006	22.73% [-0.37%; 41.40%]
SGLT2 inhibitor	5 (12.50 %)	14 (63.64 %)	<0.001	51.14% [31.21%; 78.49%]
GLP1RA	0 (0 %)	1 (4.55 %)	0.386	4.55% [-15.80%; 17.59%]
Sulfonylurea	0 (0 %)	1 (4.55 %)	0.386	4.55% [-15.80%; 17.59%]
DPP4 inhibitor	0 (0 %)	5 (22.73 %)	0.006	22.73% [-0.37%; 41.40%]
Insulin therapy	0 (0 %)	5 (22.73 %)	0.006	22.73% [-0.37%; 41.40%]
Prednisolon	35 (100 %)	22 (100 %)	>0.999	0.00% [-12.32%; 18.50%]
Tacrolimus	33 (94.29 %)	22 (100 %)	0.518	5.71% [-9.10%; 24.80%]
Everolimus	17 (48.57 %)	14 (63.64 %)	0.290	15.06% [-9.84%; 43.61%]
IMPDH inhibitor	17 (48.57 %)	8 (36.36 %)	0.420	12.21% [-16.15%; 37.32%]
<sup>1</sup> Median [25%; 75%]; n (%)				
<sup>2</sup> Mann-Whitney-Test or Fisher's exact test				
<sup>3</sup> Hodges-Lehmann estimation or Newcombe-Wilson score with continuity correction [95% CI]				

BMI: body mass index; DPP4: dipeptidyl peptidase 4; GLP1RA: glucagon-Like peptide-1 receptor agonist; HbA1c: hemoglobin A1c; IMPDH: inosine monophosphate dehydrogenase; SGLT2: Sodium-glucose cotransporter-2; T2D: type 2 diabetes

**Supplementary Table S5.** Age and BMI adjusted p-values in the human heart cohorts

Respirometry state	p-value (Control vs. T2D) adjusted for <sup>1</sup>	
	Not adjusted	Age + BMI
[HBA] <sub>p</sub>	0.279	0.533
[KL] <sub>p</sub>	0.001	0.004
[KL+ACA] <sub>p</sub>	<0.001	0.005
[F] <sub>L</sub>	0.484	0.354
[F] <sub>p</sub>	0.358	0.325
[FN] <sub>p</sub>	0.291	0.344
[FNS] <sub>p</sub>	0.178	0.213
[FNS] <sub>L</sub>	0.273	0.187
[FNS] <sub>E</sub>	0.324	0.427
[HBA] <sub>p</sub> /[FNS] <sub>p</sub>	0.915	0.668
[KL] <sub>p</sub> /[FNS] <sub>p</sub>	0.264	0.416
[KL+ACA] <sub>p</sub> /[FNS] <sub>p</sub>	0.014	0.066
[KL] <sub>p</sub> /[KL+ACA] <sub>p</sub>	0.043	0.025
<sup>1</sup> Multiple linear regression using the least squares method.		

ACA: acetoacetate; BMI: body mass index; E: electron transport chain capacity (noncoupled) mitochondrial respiration state; F: fatty acids; HBA:  $\beta$ -hydroxybutyrate; KL: ketolysis; L: leak mitochondrial respiration state; N: NADH-linked substrates; p: phosphorylating (coupled) mitochondrial respiration state; S: succinate; T2D: type 2 diabetes.



**Supplementary Table S6.** Characteristics of human participants in skeletal muscle cohorts

Characteristic	Control, N = 7 <sup>1</sup>	T2D, N = 13 <sup>1</sup>	p-value <sup>2</sup>	Difference <sup>3</sup>
Age (years)	52.2 [36.7; 58.3]	58.0 [46.4; 67.8]	0.211	7.2 [-5.0; 20.6]
Sex (% male)	4 (57%)	9 (69%)	0.651	12.09% [-30.09%; 55.50%]
BMI (kg/m <sup>2</sup> )	24.00 [21.70; 34.60]	32.10 [26.70; 37.35]	0.189	4.60 [-2.40; 11.30]
HbA1c (%)	5.20 [5.00; 5.20]	6.90 [5.90; 7.90]	<0.001	1.70 [0.80; 2.90]
Free fatty acids (μmol/L)	411 [382; 651]	553 [350; 742]	0.711	43.5 [-196.0; 272.0]
OGIS index (ml min <sup>-1</sup> m <sup>-2</sup> )	384.0 [361.8; 393.5]	290.0 [232.0; 327.5]	<0.001	-92.0 [-146.0; -50.0]
Metformin	0 (0%)	6 (46%)	0.052	46.15% [18.40%; 97.06%]
SLGT2 inhibitor	0 (0%)	3 (23%)	0.521	23.08% [-7.89%; 70.13%]
GLP1RA	0 (0%)	1 (7.7%)	1.000	7.69% [-22.56%; 52.20%]
Sulfonylurea	0 (0%)	1 (7.7%)	1.000	7.69% [-22.56%; 52.20%]
DPP4 inhibitor	0 (0%)	1 (7.7%)	1.000	7.69% [-22.56%; 52.20%]
Alpha-glucosidase inhibitor	0 (0%)	1 (7.7%)	1.000	7.69% [-22.56%; 52.20%]
Insulin therapy	0 (0%)	1 (7.7%)	1.000	7.69% [-22.56%; 52.20%]
<sup>1</sup> Median [25%; 75%]; n (%)				
<sup>2</sup> Mann-Whitney-Test or Fisher's exact test				
<sup>3</sup> Hodges-Lehmann estimation or Newcombe-Wilson score with continuity correction [95% CI]				

BMI: body mass index; DPP4: dipeptidyl peptidase IV; GLP1RA: glucagon-like peptide-1 (GLP-1) receptor agonist; HbA1c: hemoglobin A1c; OGIS: oral glucose insulin sensitivity; SGLT2: Sodium-glucose cotransporter-2; T2D: type 2 diabetes.

**Supplementary Table S7.** Age and BMI adjusted p-values in the human skeletal muscle cohorts

Respirometry state	p-value (Control vs. T2D) adjusted for <sup>1</sup>	
	Not adjusted	Age + BMI
[HBA] <sub>P</sub>	0.237	0.134
[KL] <sub>P</sub>	0.042	0.061
[KL+ACA] <sub>P</sub>	0.005	0.014
[N] <sub>P</sub>	0.616	0.318
[NS] <sub>P</sub>	0.469	0.311
[NS] <sub>E</sub>	0.855	0.803
[HBA] <sub>P</sub> /[NS] <sub>P</sub>	0.034	0.086
[KL] <sub>P</sub> /[NS] <sub>P</sub>	<0.001	<0.001
[KL+ACA] <sub>P</sub> /[NS] <sub>P</sub>	<0.001	<0.001
[KL] <sub>P</sub> /[KL+ACA] <sub>P</sub>	0.038	0.095
<sup>1</sup> Multiple linear regression using the least squares method.		

ACA: acetoacetate; BMI: body mass index; E: electron transport chain capacity (noncoupled) mitochondrial respiration state; HBA: β-hydroxybutyrate; KL: ketolysis; L: leak mitochondrial respiration state; N: NADH-linked substrates; P: phosphorylating (coupled) mitochondrial respiration state; S: succinate; T2D: type 2 diabetes.

**Supplementary Table S8.** Characteristics of DIO vs. Control mice

Characteristic	Control, N = 10 <sup>1</sup>	DIO, N = 12 <sup>1</sup>	p-value <sup>2</sup>
Age (weeks)	35 [34; 36]	36 [34; 37]	0.266
Sex (% male)	10 (100%)	12 (100%)	n/a
Body weight (g)	34.3 [31.8; 35.0]	49.3 [47.2; 56.7]	<0.001
Blood glucose [mg/dL]	278 [242; 325]	360 [306; 379]	0.002
Insulin [ng/mL]	0.41 [0.36; 0.61]	2.32 [0.87; 4.11]	0.002
<sup>1</sup> Median [25%; 75%]; n (%)			
<sup>2</sup> Mann-Whitney-Test			

DIO: diet-induced obesity.

**Supplementary Table S9.** Characteristics of participants in liver cohorts

Characteristic	No MASLD, N = 5 <sup>1</sup>	MASLD, N = 11 <sup>1</sup>	p-value <sup>2</sup>	Difference <sup>3</sup>
Age (years)	34.0 [29.0; 45.5]	41.0 [36.0; 49.0]	0.137	7.0 [-5.0; 20.0]
Sex (% male)	0 (0%)	3 (27%)	0.509	27.27% [-6.19%; 84.56%]
BMI (kg/m <sup>2</sup> )	45.00 [42.32; 51.27]	46.28 [41.70; 51.83]	0.913	0.22 [-6.58; 6.83]
Type 2 Diabetes status:			0.333	
<i>Normoglycemic</i>	4 (80%)	4 (36%)	0.282	43.64% [-15.84%; 74.21%]
<i>Prediabetes</i>	1 (20%)	5 (45%)	0.588	25.45% [-10.01%; 82.54%]
<i>Type 2 diabetes</i>	0 (0%)	2 (18%)	>0.999	18.18% [-15.93%; 73.93%]
HbA1c (%)	5.40 [4.60; 5.75]	5.90 [5.40; 6.10]	0.064	0.50 [-0.10; 0.40]
FPG (mg/dl)	87.90 [81.75; 90.15]	94.20 [84.00; 99.60]	0.065	6.30 [-2.90; 18.80]
Free fatty acids (μmol/L)	801 [655; 915]	688 [579; 922]	0.679	-62.50 [-293; 182]
Grade of steatosis (0-3)	0 [0; 0]	2 [1; 3]	<0.001	2 [1; 3]
Lobular inflammation (0-3)	1 [1; 2]	2 [1; 2]	0.420	0 [0; 1]
Hepatocellular ballooning (0-2)	0 [0; 0]	1 [0; 1]	0.017	1 [0; 2]
Total NAS (0-8)	1 [1; 2]	5 [3; 5]	<0.001	4 [2; 4]
<sup>1</sup> Median [25%; 75%]; n (%)				
<sup>2</sup> Mann-Whitney-Test or Fisher's exact test				
<sup>3</sup> Hodges-Lehmann estimation or Newcombe-Wilson score with continuity correction [95% CI]				

BMI: body mass index; FPG: fasting plasma glucose (capillary); HbA1c: hemoglobin A1c; MASLD: metabolic dysfunction-associated steatotic liver disease; NAS: non-alcoholic fatty liver disease (NAFLD) activity score.

**Supplementary Table S10.** Age and BMI adjusted p-values in the human liver cohorts

Respirometry state	p-value (No MASLD vs. MASLD) adjusted for <sup>1</sup>	
	Not adjusted	Age + BMI
[N] <sub>L</sub>	0.093	0.172
[N] <sub>P</sub>	0.998	0.861
[NS] <sub>P</sub>	0.354	0.655
[NS] <sub>E</sub>	0.398	0.764
[HBA] <sub>P</sub> /[N] <sub>P</sub>	0.002	0.017
[HBA] <sub>P</sub> /[NS] <sub>P</sub>	0.012	0.020
<sup>1</sup> Multiple linear regression using the least squares method.		

BMI: body mass index; <sub>E</sub>: electron transport chain capacity (noncoupled) mitochondrial respiration state; HBA: β-hydroxybutyrate; MASLD: metabolic dysfunction-associated steatotic liver disease; N: NADH-linked substrates; <sub>P</sub>: phosphorylating (coupled) mitochondrial respiration state; S: succinate.

## References

1. Benjamini Y, Krieger AM, Yekutieli D. Adaptive linear step-up procedures that control the false discovery rate. *Biometrika* 2006; **93**(3): 491-507.
2. Pafili K, Kahl S, Mastrototaro L, et al. Mitochondrial respiration is decreased in visceral but not subcutaneous adipose tissue in obese individuals with fatty liver disease. *J Hepatol* 2022; **77**(6): 1504-14.